Atmos. Chem. Phys. Discuss., doi:10.5194/acp-2016-499, 2016
Manuscript under review for journal Atmos. Chem. Phys.
Published: 8 July 2016

Atmospheric Chemistry and Physics Discussions
Open Access

Application of a new scheme of cloud base droplet nucleation in a Spectral (bin) Microphysics cloud model: sensitivity to aerosol concentrations

E. Ilotoviz and A. Khain

Department of Atmospheric Sciences, The Hebrew University of Jerusalem, Israel

Submitted to Atmos. Chem. Phys. Discuss.

June 2016

Communicating author: Alexander Khain, Department of Atmospheric Sciences, The Hebrew University of Jerusalem, Israel, email: alexander.khain@mail.huji.ac.il

Atmos. Chem. Phys. Discuss., doi:10.5194/acp-2016-499, 2016
Manuscript under review for journal Atmos. Chem. Phys.
Published: 8 July 2016

Abstract

A new scheme of droplet nucleation at cloud base is implemented into the Hebrew University cloud model (HUCM) with spectral (bin) microphysics. In this scheme, supersaturation maximum S_{max} near cloud base is calculated using theoretical results according to which $S_{\max} \sim W^{3/4} N_d^{-1/2}$, where W is the vertical velocity at cloud base and N_d is droplet concentration. Microphysical cloud structure obtained in the simulations of a mid-latitude hail storm using the new scheme is compared with that obtained in the standard approach, in which droplet nucleation is calculated using the values of supersaturation calculated in grid points. The simulations were performed with high and low concentrations of cloud condensational nuclei and different slope parameters in expression for the activity CCN spectra. It is shown that the new scheme substantially improves the vertical profile of droplet concentration shifting the concentration maximum to cloud base. The effect of calculation of droplet concentration using the analytical prediction of S_{max} is especially significant in cases of high CCN concentration. Application of the new approach in cases of low CCN concentration does not change cloud microphysics significantly. It is shown that the shape of CCN size distribution on cloud microphysics is not less important than the effect of total CCN concentration. It is shown that the smallest CCN with diameters less than about 0.015 μm have a substantial effect on microphysics of deep convective clouds.

Key words: cloud-aerosol interaction, droplet nucleation at cloud base, spectral bin microphysics

Atmos. Chem. Phys. Discuss., doi:10.5194/acp-2016-499, 2016
Manuscript under review for journal Atmos. Chem. Phys.
Published: 8 July 2016

Atmospheric Chemistry and Physics
Discussions

1. Introduction

Droplet concentration is the key microphysical parameter that affects precipitation formation, and radiative cloud properties (Pruppacher and Klett, 1997). The maximum value of supersaturation near cloud base (S_{max}) determines the amount of activated cloud condensational nuclei (CCN) and, consequently, droplet concentration. The maximum supersaturation is reached a few tens of meters above cloud base [*Rogers and Yau*, 1996; Pinsky et al. 2013]. The vertical grid spacing of most cloud-resolving models is too coarse to resolve this maximum. This can lead to errors in determination of droplet concentration. Therefore, it is desirable to parameterize the process of droplet nucleation near cloud base. One approach to the parameterization is based on lookup tables developed using precise 1D parcel models (e.g., Segal and Khain, 2006). The other approach is based on analytical calculation of supersaturation maximum, $S_{\max}$, near cloud base. This approach has been developing in several studies using one or another assumptions concerning CCN activity spectra [*Ghan et al.*, 1993, 1997; *Bedos et al.*, 1996; *Abdul-Razzak et al.*, 1998; *Cohard et al.*, 1998; *Abdul-Razzak and Ghan*, 2000; *Fountoukis*, 2005; *Shipway and Abel*, 2010]. The results and a comparison of these approaches are presented by *Ghan et al. [2011]*. Note that the calculation of the supersaturation maximum is a complicated mathematical problem [*Khvorostyanov and Curry*, 2006] that is typically reduced to solving an integro-differential equation which uses different expressions for CCN activity spectra. The parameters of activity CCN spectra, as well as the concentration and shape of the CCN size distributions, are often prescribed in atmospheric models and assumed to be invariant over time.

Pinsky et al. [2012] proposed a simple method of calculation of $S_{\max}$ near cloud base and, accordingly, droplet concentration at cloud base at any CCN spectra. The detailed test of the

Atmos. Chem. Phys. Discuss., doi:10.5194/acp-2016-499, 2016
Manuscript under review for journal Atmos. Chem. Phys.
Published: 8 July 2016

method showed very good agreement with exact results (obtained using a 1-D model) as regards of the values of $S_{\max}$ and droplet concentration.

In this study we investigate the effects of the new method for calculating droplet concentration on the microphysics of mid-latitude deep convective clouds (hail storm) using the Hebrew University Cloud model (HUCM) with spectral-bin microphysics (SBM). The effect of the new approach (NA, hereafter) is investigated in simulations with different parameters of CCN activity spectra.

2. Model description

The HUCM is a 2-D, nonhydrostatic SBM model, which microphysics is based on solving a system of equations for size distributions of liquid drops, three types of pristine ice crystals (plates, columns, and dendrites), snow/aggregates, graupel, hail and partially frozen or "freezing drops". Each size distribution is discretized into 43 mass-doubling bins, with the smallest bin equivalent to the mass of a liquid droplet of radius 2 μm. Aerosol particles playing the role of CCN are also defined on a mass grid containing 43 mass bins. The size of dry CCNs ranges from 0.005 μm to 2 μm.

Primary nucleation of each ice crystal type is described using Meyers et al. [1992] parameterization. The type of ice crystals is determined depending on temperature range where the particles arise (Takahashi et al. 1991). Secondary ice generation is accounted for during riming (Hallett and Mossop 1974). Collisions are described by solving the stochastic collection equations for the corresponding size distributions using the Bott (1998) method. Height-dependent, gravitational collision kernels for drop-drop and drop-graupel interactions are from Pinsky et al. (2001) and Khain et al. (2001); those for collisions between ice crystals are from

Atmos. Chem. Phys. Discuss., doi:10.5194/acp-2016-499, 2016
Manuscript under review for journal Atmos. Chem. Phys.
Published: 8 July 2016

Khain and Sednev (1995) and Khain et al. (2004). The latter studies include the dependence of particle mass on the ice crystal cross-section. The effects of turbulence on collisions between cloud drops are included (Benmoshe et al. 2012). The collision kernels depend on the turbulence intensity and changes in time and space.

The time-dependent melting of snow, graupel, and hail as well as shedding of water from hail follows Phillips et al. (2007). We have implemented liquid water mass in these hydrometeor particles that is advected and sediment similarly to the mass of the corresponding particles. As a result, these particles are characterized by their total mass and by the mass of liquid water (i.e., the liquid water mass fraction). The liquid water fraction increases during melting. As soon as it exceeds ~95%, the melting particles are converted to raindrops. Process of time dependent freezing is described according to Phillips et al. (2014, 2015). Process of freezing consists of two stages. The first nucleation stage is described using the parameterization of immersion drop freezing proposed by Vali (1994) and Bigg (1953). Drops with radii below 80 μm that freeze are assigned to plates, whereas larger drops undergoing freezing are assigned to freezing drops. The freezing drops consist of a core of liquid water surrounded by an ice envelope. Time-dependent freezing of liquid within freezing drops is calculated by solving heat balance equations that take into account the effects of accretion of supercooled drops and ice particles. Collision between freezing drops and other hydrometeors lead either to the freezing drops category if the freezing drop is larger than its counterpart, or otherwise, the resulting particle is assigned to the type of counterpart. Once the liquid water fraction in a freezing drop becomes less than some minimal value (<1%) it is converted to a hailstone. Hail can grow either by dry growth or by wet growth (*Phillips et al.* 2014, 2015). Accordingly, liquid water is allowed in hail and graupel particles at both positive and negative temperatures. The shedding of water in wet growth is also included.

Atmos. Chem. Phys. Discuss., doi:10.5194/acp-2016-499, 2016
Manuscript under review for journal Atmos. Chem. Phys.
Published: 8 July 2016

Atmospheric Chemistry and Physics Discussions

Water accreted onto aggregates (snow) freezes immediately at temperatures below $0\,^0C$, where it then contributes to the rimed fraction. This rimed mass distribution is advected and sediment similarly to the snow masses. Riming mass increases the density of the aggregates. As the bulk density of snow in a certain mass bin exceeds a critical value (0.2 $g\ cm^{-3}$), the snow from this bin is converted into graupel. The appearance of water on the surface of hailstones as well as increases in the rimed fraction of snowflakes affects the particle fall velocities and coalescence efficiencies.

The initial size distribution of CCN (at t=0) is calculated using the empirical dependence (i.e., the Twomey formula) of concentration N_{ccn} of activated CCN on supersaturation S_w (in %) $N_{ccn} = N_o S_w^k$, where N_o and k are the measured constants (see [*Khain et al.*, 2000] for details). The obtained aerosol size distribution is corrected in zones of very small and very large CCN, that is, in size ranges where the Twomey formula is invalid. At t>0 the prognostic equation for the size distribution of non-activated CCN is solved. Using the value of S calculated at each time-step and in each grid point, the critical radius of CCN particles was determined according to the Köhler theory. The CCNs with radii exceeding the critical value are activated and new droplets are nucleated. The corresponding bins of the CCN size distributions become empty.

In the new approach (NA) nucleation of droplets near cloud base is performed following *Pinsky et al.* [2012] , who derived the following relationship between supersaturation maximum near cloud base and vertical velocity w and droplet concentration N_d:

$$S_{\max} = C\, w^{3/4} N_d^{-1/2} \qquad (1)$$

where coefficient C slightly depends on the thermodynamical parameters only (see **Table 1** for notations). Since the droplet concentration is equal to the concentration of CCN activated at $S_w = S_{\max}$, the droplet concentration can be calculated as

$$N_d = \int_{r_{n\_cr}(S_{\max})}^{\infty} f(r_n) dr_n \tag{2}$$

where $f(r_n)$ is a size distribution of dry aerosol particles and r_{n_cr} is critical radius of aerosol activated under $S_{\max}$. This radius relates to $S_{\max}$ as $r_{n\_cr} = \frac{A}{3}\left(\frac{4}{BS_{\max}^2}\right)^{1/3}$, where coefficients A and B are the coefficients of the Köhler equation. From Eqs. (1-2) one can obtain equation for $S_{\max}$:

$$S_{\max}\left[\int_{r_{n\_cr}(S_{\max})}^{\infty} f(r_n) dr_n\right]^{1/2} = C\, w^{3/4} \tag{3}$$

Eq. (3) was used to calculate $S_{\max}$, r_{n_cr} and concentration of nucleated droplets.

3. Design of simulations

All simulations were performed within a computational domain of 153.9 km x 19.2 km, and a grid spacing of 300 m in the horizontal direction and 100 m in the vertical direction. A new microphysical scheme was tested in simulations of a thunderstorm observed in Villingen-Schwenningen, southwest Germany, on 28 June 2006**.** Meteorological conditions (including sounding) of this storm were described by *Khain et al.* [2011]. The background wind direction was quasi-2-D, which simplified the prescription of the background wind profile in the 2-D model. The wind speed increased with height from ~10 $m\,s^{-1}$ in the lower atmosphere to about 20 $m\,s^{-1}$ at levels of 100-200 mb. We used a surface temperature of 22.9°C, which was similar to the daily maximum air temperature near the surface in Villingen- Schwenningen at 15 UTC. The relative humidity near the ground was high (~85%), which led to a low lifting condensation level of about 890 m. The freezing level was located around 3.5 km. The observed maximum diameter of hailstones was about 5 cm.

The convection was initiated by a cool pool that triggered convective cloud formation. This type of storm triggering is used traditionally in simulations of long-lasting convection [*Rotunno and Klemp*, 1985].

Three sets of simulations were produced. In each set, the simulations were performed in two versions: the standard approach (ST, hereafter), where the critical CCN radius was calculated using a supersaturation calculated at the grid points, and using the NA, where the critical CCN radius and $S_{\max}$ were determined from Eq. (3).

The first set of simulations aims at the comparison of the microphysics in the NA and the ST in cases of high (N_0 =3500 cm^{-3}) and small (N_0 =100 cm^{-3}) CCN concentrations. Minimum radii of CCN were set equal to 0.015 μm and 0.0125 μm, respectively. Similar CCN size distributions were used by Khain et al (2011). These simulations are referred to as E3500, E100 (ST) and EN3500, and EN100 (NA), respectively.

In *the second set of simulations* the smallest CCN were added into the aerosol particle (AP) spectra. The large impact of the smallest CCN in the formation of ice crystals in cloud anvils was shown by Khain et al. [2012]. In this set the minimum CCN radii were taken equal to 0.006 μm and 0.003 μm in cases of high and low CCN concentrations, respectively. These simulations are referred to as E3500-S, EN3500-S, E100-S and EN100-S.

In these two sets of simulations the slope parameter k was assumed equal to 0.9.

Atmos. Chem. Phys. Discuss., doi:10.5194/acp-2016-499, 2016
Manuscript under review for journal Atmos. Chem. Phys.
Published: 8 July 2016

The third set of simulations was similar to the second one, but the slope parameter was taken k =0.5. In many studies investigating effects of aerosols on cloud microphysics only parameter N_0 is changed. However, the slope parameter determines the relationship between concentration of smaller and larger CCN, so concentration of nucleated droplets also depends on the slope parameter. The simulations of the third set are referred to as E3500-S-05, EN3500-S-05, E100-S-05 and EN100-S-05. Size distributions of CCN in these experiments are shown in **Figure 1**.

CCN concentrations in different experiments are presented in **Table 2**. Although the difference between total aerosol concentrations is not large, in case k=0.5 the CCN size distribution contains more large CCN, and less small CCN. These size distributions were assumed within the lower 2-km layer. Above this level, the CCN concentration in each mass bin was decreased exponentially with height. Above 8 km, the CCN concentration was set constant.

4. Results of simulations

4.1 Vertical profiles of supersaturation near cloud base

The model calculates supersaturation at the model levels which typically do not coincide with the cloud base level where supersaturation S_w=0. We treat the first level where $S_w > 0$ as the cloud base. Since the supersaturation maximum is reached not far from cloud base level, we attribute the values of $S_{\max}$ to this level. Correspondingly, the difference between NA and ST in the droplet concentrations is also attributed to this level. **Figure 2** presents two examples of vertical profiles of supersaturation (%) near cloud base in the ST and the NA simulations. The profiles of supersaturation chosen when the vertical velocities at cloud

Atmos. Chem. Phys. Discuss., doi:10.5194/acp-2016-499, 2016
Manuscript under review for journal Atmos. Chem. Phys.
Published: 8 July 2016

base were 0.5 ms^{-1} and 1 ms^{-1}, respectively. It is natural that the values of $S_{\max}$ are larger in cases of low CCN concentration as compared to the high CCN case. For goals of the present study, the more interesting is that the values of $S_{\max}$ calculated using NA are substantially larger than S_w calculated at model level associated to the cloud base in the ST. The difference between NA and ST in the supersaturation values leads to a substantial difference in the droplet concentrations, especially in cases of high CCN concentration. Calculation of $S_{\max}$ at cloud base changes the vertical profile of supersaturation in the layer just above cloud base. While in the ST supersaturation changes only slightly or even increase with height within the 100-200 m above cloud base, in the NA supersaturation decreases within this layer above supersaturation maximum in agreement with the theory (Rogers and Yau, 1989, Pinsky et al, 2012, 2013).

4.2 High CCN concentration

In this section we compare the results for three pairs of simulations in which clouds were developed in a highly polluted atmosphere. **Figure 3** shows the fields of droplet concentration N_d at the developing stage of the cloud evolution in E3500-S-0.5 (a), EN3500-S-0.5 (b), E3500-S (c) and EN3500-S (d). The maximum N_d in a NA is reached at cloud base, which makes the cloud base well pronounced. The difference between droplet concentrations in the ST and the NA experiments decreases with height. Larger droplet concentration is reached in simulations with the slope factor k=0.5 of the CCN activity spectrum. This can be attributed to the fact that in case of k=0.9 aerosol spectrum contains more smallest CCN which are not activated at cloud base.

Vertical profiles of the maximum values of droplet concentration and of cloud water content (CWC) are presented in **Figure 4.** In the NA the N_d maximum decreases with height beginning with the cloud base level. This behavior of $N_d(z)$ is obviously more realistic than in ST, where the N_d maximum slightly increases with height up to an altitude of 4 km. This increase in the N_d maximum in the ST is caused by in-cloud activation of CCN which were not activated at cloud base. In the NA, these CCN were activated at cloud base. There is, therefore, a negative feedback in the supersaturation-droplet concentration relationship: an underestimation of supersaturation at the low levels in the ST simulations leads to the underestimation of droplet concentration and to the corresponding increase in supersaturation. Above a height of 4 km, droplet concentrations in both cases turn out to be similar, regardless of which approach is used leading to comparatively small differences in ice microphysics. The results indicate that in those models where droplet nucleation is calculated only at cloud base, the correct calculation of $S_{\max}$ at cloud base is strictly necessary to obtain reasonable values of N_d in clouds.

The effect of the smallest CCN on N_d is seen above 6 km altitude by comparison of profiles in E3500 (or EN3500) and E3500S (or EN3500S) (Fig. 4a). These smallest CCN are activated and produce additional droplets by in-cloud nucleation caused by an increase in supersaturation due to a decrease in CWC (Fig. 4b) and an increase in vertical velocity (not shown). The increase in N_d by activation at high levels and its effect on concentration of ice crystals in cloud anvils of deep convective clouds was also reported by Khain et al. (2012).

Fig. 4a shows also that N_d is very sensitive to slope parameter. The maximum N_d reached at cloud base is about 1100 cm^{-3} in EN3500-S-05 (k=0.5) as compared to ~550 cm^{-3} in EN3500-S (k=0.9). Vertical profiles of CWC (Fig. 4b) are typical of deep convective clouds developing in the highly polluted environment: CWC is large and has maximum at about 5 km, i.e. at quite high altitude.

The difference in concentration of small droplets at higher levels induced by nucleation of smallest droplets results in a dramatic difference in the concentration of ice crystals in cloud anvils. **Figure 5a** shows the vertical profiles of maximum concentration of plate crystals (in HUCM homogeneous freezing leads to formation of plates) averaged over the mature stage of cloud evolution (from 4860 to 5460s). The number concentration of ice crystals in E3500 and EN3500 (in which there are no the smallest CCN in the initial CCN spectrum) is by factor of 5 lower than in simulations containing these smallest CCN. The results show that ice crystal concentration in the NA is higher only slightly than in the ST simulations. Thus, in the simulations, the concentration of ice crystals in cloud anvils is very sensitive to the concentration of smallest CCN in the CCN spectra and is substantially less sensitive to larger CCN, which are activated at cloud base. Fig. 5b shows that this conclusion is valid for entire period of the simulation. The concentration of plates increased when the NA was applied (**Figure 5b**).

Figure 6 shows the vertical profiles of time averaged maximal mass contents of ice crystals, snow, graupel and hail+freezing drops at the storm mature stage. The maximum difference between ice crystal mass contents takes place at ~10-11 km, where ice crystals are caused by homogeneous freezing. The most pronounced effect of the NA is an increase in the accretion rate. In agreement with results of simulations of aerosol effects on ice microstructure of deep convective clouds (Khain 2009; Tao et al. 2012; Khain et al. 2016), the intensification of riming leads to the decrease in the snow mass content and to the increase in the mass contents of graupel and hail (Fig.6b-d). The existence of the smallest CCN concentration leads to an increase in the differences between the NA and the ST.

4.3 Low CCN concentration

In this section we compare the results for three pairs of simulations: E100 and EN100, E100-S and EN100-S, and E100-S-0.5, and EN100-S-0.5 in which clouds were developed in the low CCN concentration atmosphere. After the first 35 min of cloud evolution, the cloud base is located at 700-800 m altitude and T=16.8℃ at this level.

The fields of droplet concentration N_d in different experiments at the developing stage of the cloud evolution are shown in **Figure 7**. The maximum N_d in a NA is reached at cloud base, which makes the cloud base well pronounced. The difference in droplet concentrations in the ST and the NA experiments decreases with height**.** Although the difference is N_d between the NA and ST is very pronounced, the absolute difference is not large, of about 20 cm^{-3}. This low N_d determines a very maritime structure of clouds in both cases.

Figure 8 shows vertical profiles of the maximum values of droplet concentration and cloud water content (CWC) averaged over the time period of 2100 – 2700s. Both the droplet concentration and CWC are larger in the NA as compared to the ST. Since clouds are very maritime, droplet collisions are efficient and warm rain sharply decreases the droplet concentration above 2-3 km. CWC is larger in the NA.

In agreement with the theory (Pinsky et al. 2012), the supersaturation maximum in case of low concentration is reached at larger distance above cloud base than in the case of high CCN concentration. As a result, $S_{\max}$ calculated using Eq. (3) is closer to the supersaturation calculated in model grid points than in case of high CCN concentration. So the main difference between droplet concentrations in Fig. 8 is caused by the difference in the shape of CCN size distribution (different slope parameters).

The smallest CCNs lead to a substantial increase in the droplet concentration above 3-4 km (Fig. 8a). Efficient rain formation (seen by the sharp decrease in the CWC) decreases the droplet concentration. As a result, the supersaturation increases and leads to in-cloud nucleation of the smallest aerosols already at distances close to cloud base. However, because of the low concentration of CCN the amount of new nucleated droplets in the simulations was only about 5 cm^{-3}.

Figure 9 presents the vertical profiles of maximum mass density of total ice crystals, snow, graupel and hail + freezing drops at the mature stage of cloud evolution. Comparison with Fig. 6 shows that at the exception of snow, the mass contents of different ice hydrometeors in case of low CCN concentration are much lower than in case of high CCN concentration. The profiles of ice hydrometeors in the NA and the ST are quite similar. The effects of the smallest CCN and the shape of CCN size spectra on droplet concentration and the concentration on ice microphysics are much stronger than the effect of additional droplets nucleating at cloud base in the NA. The reason for this effect was mentioned above.

The increase in CCN (and droplet concentration) leads to a decrease in the mass contents of ice crystals and snow, but to the increase in mass content of graupel and hail.

The effects of the smallest CCN are similar to that in the high CCN concentration. Activation of the smallest CCN leads to more intense riming, larger ice crystal concentration in cloud anvil and larger masses of graupel and hail.

4.3 The impact on precipitation

Figure 10a shows the accumulated rain at surface in the polluted cases. Accumulated rain is maximal in the EN3500-S-0.5, where effect of small CCNs is combined to the effect of comparatively large amount of large CCN. This synergetic effect of the smallest and large CCN

Atmos. Chem. Phys. Discuss., doi:10.5194/acp-2016-499, 2016
Manuscript under review for journal Atmos. Chem. Phys.
Published: 8 July 2016

Atmospheric Chemistry and Physics Discussions

is described by Khain et al. (2011). In the most simulations, the masses of accumulated rain are quite similar.

Figure 10b shows that the accumulated rain in case of low aerosol concentration is lower than in case of high CCN concentration in agreement with many previous studies. Accumulated rain in the NA turns out to be quite close to that in the ST. Main difference in the values of accumulated rain in the low CCN concentration case is caused by effects of smallest aerosols and shape of the CCN size distribution.

Amount of hail at the surface in polluted cases is slightly higher in EN3500-S-0.5 as compared to E3500-S-0.5 (**Figure 10c**). We attribute this effect to higher rate of riming in EN3500-S-0.5 due to higher amount of supercoold water. There is no significant differences in the other polluted cases. In clean cases the amount of hail at surface is lower than in polluted cases (**Figure 10d**). An increase in hail amount at the surface in EN100-S as compared to E100-S can be attributed to the intensification of hail growth caused by contribution of additional small droplets to the riming process.

5. Conclusions

Sensitivity of microphysics of deep convective clouds to the concentration of aerosols and to the shape of aerosol size distribution is investigated using a new version of a 2-D Spectral (bin) Microphysics cloud model (HUCM). One of new components of the model is the calculation of maximum supersaturation at cloud base using analytical expression derived by *Pinsky et al.* [2012]. The cloud microphysical structure obtained using this expression is compared with that obtained when supersaturation was calculated in model grid points.

The goal of the study was twofold: a) to test effects of the improved calculation of supersaturation maximum near cloud base (new approach-NA) at different aerosol loadings and

Atmos. Chem. Phys. Discuss., doi:10.5194/acp-2016-499, 2016
Manuscript under review for journal Atmos. Chem. Phys.
Published: 8 July 2016

b) to evaluate sensitivity of cloud microphysics to concentration and shape of size distribution of aerosol particles. Shape of the CCN size distributions was changed by changing of the slope parameter in the expression for activity spectrum (the values of k=0.5 and k=0.8 were used) and by adding the smallest CCN with radii below 0.015 μm.

It was shown that the droplet concentration field in the NA is substantially more realistic: the maximum of droplet concentration was located near cloud base, which made the cloud base more pronounced. The improvement of the representation of vertical profile of the droplet concentration is especially significant in case of high CCN concentration. The latter can be attributed to the fact that in cases of high CCN concentration, errors in the calculation of supersaturation lead to substantial errors in the value of droplet concentration. In the ST, the supersaturation calculated in grid points near cloud base turned out to be substantially underestimated as compared to the theoretically determined supersaturation maximum. This led to a substantial underestimation of the droplet concentration near cloud base in the ST. Thus, even in case of 100 m vertical resolution, the utilization of analytical expressions for $S_{\max}$ is necessary.

The error in the calculation of droplet concentration near cloud base in HUCM is compensated to a significant extent by in-cloud nucleation. The models with microphysical schemes that do not describe in-cloud droplet nucleation have to include the calculation of $S_{\max}$ at cloud base to avoid large errors in the simulation of the microphysical cloud structure.

Despite the fact that the error in the calculation of droplet concentration near cloud base is partially compensated in the ST by in-cloud nucleation, the concentration of droplets in the NA was higher than in the ST at higher levels as well. The higher concentration of droplets in the NA leads to more intense riming, larger maximum values of graupel and hail mass contents and to increased hail size. It also leads to larger masses of ice crystals in cloud anvils. In this respect the effect of NA is similar to that of an increase in the CCN concentration.

In cases of low CCN concentration, the improvement of representation of the droplet concentration above cloud base has only a slight effect on cloud microphysics. This result can be attributed to the fact that more accurate calculation of droplet concentration leads to a comparatively small increase in the droplet concentration just because the available CCN concentration is low. As a result, intense warm rain rapidly arises in both the NA and in the ST.

Both in cases of low and high CCN concentration, the main differences in ice microphysics is caused by the shape of CCN spectra and by existence/absence of the smallest aerosols in the CCN spectra. In cases of high CCN concentration, the effect of the smallest CCN in the NA becomes important above 5-6 km altitude where they are activated producing additional supercooled liquid droplets. The latter leads to increase in the concentration of ice crystals above the level of homogeneous freezing by factor of about 5, to doubling of maximum graupel mass and to substantial increase in the maximum of hail mass.

In case of low CCN concentration the smallest CCN also lead to an increase in the concentration and mass contents of ice crystals and to a significant increase of graupel and hail mass contents.

It was found a high sensitivity of cloud microphysics to the slope parameter of the CCN activity spectra. The effect is as strong as the change in the total CCN concentration via the change in the intercept parameter N_0. The utilization of k=0.5 instead of k=0.9 nearly doubled droplet concentration that leads to corresponding effects on cloud microphysics, in particular, to an increase in accumulated rain.

Ice precipitations at the surface are much lower than liquid precipitation. Nevertheless, hail precipitation at the surface in case of high CCN concentration is 2-3 times higher than in case of low CCN concentration in agreement with results by Khain et al. (2011) and Ilotoviz et al. (2015).

The concentrations of drops and ice crystals are important parameters determining cloud radiative properties. In this context, more accurate calculation of the concentrations using the NA should improve the accuracy of evaluation of radiative cloud properties. The proposed approach of calculation of nucleation of droplets at cloud base is simple in the utilization and computationally efficient. It can be used in cloud-resolved models with different vertical grid spacing. The utilization of cruder vertical model resolution may lead to larger errors in cases when droplet concentration at cloud base is calculated using supersaturations calculated at model grid points.

Acknowledgements

The study is supported by grant the US Department of Energy Award DE_FOA-0000647 from the U.S. Department of Energy Atmospheric System Research Program, the Binational US-Israel Science Foundation (grant 2010446), and by the Israel Science Foundation (grant 1393/14).

Appendix. List of symbols

Atmos. Chem. Phys. Discuss., doi:10.5194/acp-2016-499, 2016
Manuscript under review for journal Atmos. Chem. Phys.
Published: 8 July 2016

References

Abdul-Razzak, H., and S. J. Ghan (2000), A parameterization of aerosol activation: 2. Multiple aerosol types, *J. Geophys. Res.*, *105*(D5), 6837, doi:10.1029/1999JD901161.

Abdul-Razzak, H., S. J. Ghan, and C. Rivera-Carpio (1998), A parameterization of aerosol activation: 1. Single aerosol type, *J. Geophys. Res.*, *103*(D6), 6123, doi:10.1029/97JD03735.

Bedos, C., K. Suhre, and R. Rosset (1996), Adaptation of a cloud activation scheme to a spectral-chemical aerosol model, *Atmos. Res.*, *41*(3-4), 267–279, doi:10.1016/0169-8095(96)00014-2.

Cohard, J.-M., J.-P. Pinty, and C. Bedos (1998), Extending Twomey's Analytical Estimate of Nucleated Cloud Droplet Concentrations from CCN Spectra, *J. Atmos. Sci.*, *55*(22), 3348–3357, doi:10.1175/1520-0469(1998)055<3348:ETSAEO>2.0.CO;2.

Fountoukis, C. (2005), Continued development of a cloud droplet formation parameterization for global climate models, *J. Geophys. Res.*, *110*(D11), D11212, doi:10.1029/2004JD005591.

Ghan, S. J., C. C. Chung, and J. E. Penner (1993), A parameterization of cloud droplet nucleation part I: single aerosol type, *Atmos. Res.*, *30*(4), 198–221, doi:10.1016/0169-8095(93)90024-I.

Ghan, S. J., L. R. Leung, R. C. Easter, and H. Abdul-Razzak (1997), Prediction of cloud droplet number in a general circulation model, *J. Geophys. Res.*, *102*(D18), 21777, doi:10.1029/97JD01810.

Ghan, S. J., H. Abdul-Razzak, A. Nenes, Y. Ming, X. Liu, M. Ovchinnikov, B. Shipway, N. Meskhidze, J. Xu, and X. Shi (2011), Droplet nucleation: Physically-based parameterizations and comparative evaluation, *J. Adv. Model. Earth Syst.*, *3*(4), n/a–n/a, doi:10.1029/2011MS000074.

Heymsfield A. J., A. Bansemer, G. Heymsfield and A.O. Fierro (2009), Microphysics of maritime tropical convective updrafts at temperatures from -20 *oC to -60 oC, J. Atmos. Sci., 66, 3530-3565.*

Khain, A., M. Ovtchinnikov, M. Pinsky, A. Pokrovsky, and H. Krugliak (2000), Notes on the state-of-the-art numerical modeling of cloud microphysics, *Atmos. Res.*, *55*(3-4), 159–224, doi:10.1016/S0169-8095(00)00064-8.

Khain, A.P., D. Rosenfeld, A. Pokrovsky, U. Blahak, and A. Ryzhkov (2011), The role of CCN in precipitation and hail in a mid-latitude storm as seen in simulations using a spectral (bin) microphysics model in a 2D dynamic frame, *Atmos. Res.*, *99*(1), 129–146, doi:10.1016/j.atmosres.2010.09.015.

Khain, A.P., V. Phillips, N. Benmoshe, and a. Pokrovsky (2012), The Role of Small Soluble Aerosols in the Microphysics of Deep Clean Clouds, *J. Atmos. Sci.*, *69*(9), 2787–2807, doi:10.1175/2011JAS3649.1.

Atmos. Chem. Phys. Discuss., doi:10.5194/acp-2016-499, 2016
Manuscript under review for journal Atmos. Chem. Phys.
Published: 8 July 2016

Khain A.and B. Lynn And J. Shpund, 2016: High Resolution WRF Simulations of Hurricane Irene: Sensitivity to Aerosols and Choice of Microphysical schemes. Atmos. Research. Volume 167, 1 January 2016, 129–145.

Khvorostyanov, V. I., and J. a. Curry (2006), Aerosol size spectra and CCN activity spectra: Reconciling the lognormal, algebraic, and power laws, *J. Geophys. Res.*, *111*(D12), D12202, doi:10.1029/2005JD006532.

Meyers, M. P., P. J. DeMott, and W. R. Cotton, 1992: New primary ice-nucleation parameterizations in an explicit cloud model. J. Appl. Meteor., 31, 708–721.

Pinsky M., I. Mazin, A. Korolev and A. Khain (2012), Analytical estimation of droplet concentration at cloud base, *J. Geophys. Res*. 117, D18211, 14 PP.

Pinsky M., I.P. Mazin, A. Korolev , and A. Khain, 2013:Supersaturation and diffusional droplet growth in liquid clouds. J. Atmos. Sci. 70, 2778-2793

Pruppacher, H.R., Klett, J.D., 1997. Microphysics of Clouds and Precipitation. 2nd edn. Oxford Press, 914 p.

Rogers R. R. and Yau M. K, 1989: A Short Course in Cloud Physics, Pergamon press. 293pp.

Rosenfeld, D., U. Lohmann, G. B. Raga, C. D. O'Dowd, M. Kulmala, S. Fuzzi, A. Reissell, and M. O. Andreae (2008), Flood or drought: how do aerosols affect precipitation?, *Science*, *321*(5894), 1309–13, doi:10.1126/science.1160606.

Rotunno, R., and J. Klemp (1985), On the Rotation and Propagation of Simulated Supercell Thunderstorms, *J. Atmos. Sci.*, *42*(3), 271–292, doi:10.1175/1520-0469(1985)042<0271:OTRAPO>2.0.CO;2.

Segal Y. and Khain, A. P., 2006: Dependence of droplet concentration on aerosol conditions in different cloud types: application to droplet concentration parameterization of aerosol conditions, J. Geophys. Res. Vol. 111, D15204, doi:10.1029/2005JD006561

Shipway, B. J., and S. J. Abel (2010), Analytical estimation of cloud droplet nucleation based on an underlying aerosol population, *Atmos. Res.*, *96*(2-3), 344–355, doi:10.1016/j.atmosres.2009.10.005.

Tao W.-K., Jen-Ping Chen, Zhanqing Li, Chien Wang, Chidong Zhang (2012), Impact of Aerosols on Convective Clouds and Precipitation. *Reviews of Geophysics*. 50, Issue 2, June 2012 DOI: 10.1029/2011RG000369.

Atmos. Chem. Phys. Discuss., doi:10.5194/acp-2016-499, 2016
Manuscript under review for journal Atmos. Chem. Phys.
Published: 8 July 2016

Atmospheric Chemistry and Physics Discussions
Open Access
EGU

Table 1. List of symbols

Symbol	Description	Units
A	$\frac{2\sigma_w}{\rho_w R_v T}$	m
A_1	$\frac{g}{R_a T}\left(\frac{L_w R_a}{c_p R_v T}-1\right)$	m^{-1}
A_2	$\frac{1}{q_v}+\frac{L_w^2}{c_p R_v T^2}$	-
B	$\frac{v_n \Phi_s \varepsilon_m M_w \rho_n}{M_n \rho_w}$	-
B_1	$\frac{3}{F}\left(\frac{4\pi\rho_w}{3\rho_a}\right)^{2/3}$	$m^2 s$
C	$1.058(FA_1/3)^{3/4}\left(\frac{3\rho_a}{4\pi\rho_w A_2}\right)^{1/2}$	$m^{9/4}\ s^{-3/4}$
c_p	specific heat capacity of moist air at constant pressure	$J\ kg^{-1}K^{-1}$
D	coefficient of water vapor diffusion in the air	$m^2\ s^{-1}$
E	water vapor pressure	$N\ m^{-2}$

Atmos. Chem. Phys. Discuss., doi:10.5194/acp-2016-499, 2016
Manuscript under review for journal Atmos. Chem. Phys.
Published: 8 July 2016

e_w	saturation vapor pressure above the flat surface of water	$N\ m^{-2}$
G	acceleration of gravity	$m\ s^{-2}$
F	$\left(\frac{\rho_w L_w^2}{k_a R_v T^2} + \frac{\rho_w R_v T}{e_w(T) D}\right)$	$m^{-2}\ s$
h	$h = A_1 z$ dimensionless height	-
K	parameter of activity spectra	
k_a	coefficient of air heat conductivity	$J\ m^{-1} s^{-1} K^{-1}$
L_w	latent heat for liquid water	$J\ kg^{-1}$
M_n	molecular weight of aerosol salt	$kg\ mol^{-1}$
M_w	molecular weight of water	$kg\ mol^{-1}$
N	concentration of liquid droplets	m^{-3}
N_0	parameter of activity spectra	
P	pressure of moist air	$N\ m^{-2}$
q_v	water vapor mixing ratio (mass of water vapor per 1 kg of dry	-
q_w	liquid water mixing ratio (mass of liquid water per 1kg of dry a	-
R	liquid droplet radius	m
$r_{\max}$	drop radius at $z = z_{\max}$	m
R	$\frac{3}{FA_1 w}\left(\frac{4\pi\rho_w N A_2}{3\rho_a}\right)^{2/3}$	-
S	$S = e/e_w - 1$ supersaturation over water	-
$S_{\max}$	supersaturation maximum	-
T	absolute temperature	^{o}K

Atmos. Chem. Phys. Discuss., doi:10.5194/acp-2016-499, 2016
Manuscript under review for journal Atmos. Chem. Phys.
Published: 8 July 2016

T_C	temperature at cloud base	^oC
w	vertical velocity	m s^{-1}
z	height over condensation level	m
z_{max}	height of supersaturation maximum	m
β	parameter of activity spectra	
ε_m	soluble fraction	-
ρ_a	density of air	kg m^{-3}
ρ_N	density of a dry aerosol particle	kg m^{-3}
ρ_w	density of liquid water	kg m^{-3}
σ_w	surface tension of water-air interface	Nm^{-1}
μ	parameter of activity spectra	
ν_n	van 't Hoff factor	-

Table 2. CCN concentrations in different experiments in the boundary layer

	High CCN concentration, cm^{-3}		Low CCN concentration, cm^{-3}	
	No smallest CCN	With smallest CCN	No smallest CCN	With smallest CCN
k=0.9	840	2930	33	214
k=0.5	1552	3140	53	152

Atmos. Chem. Phys. Discuss., doi:10.5194/acp-2016-499, 2016
Manuscript under review for journal Atmos. Chem. Phys.
Published: 8 July 2016

481

482

483 # Figures

484

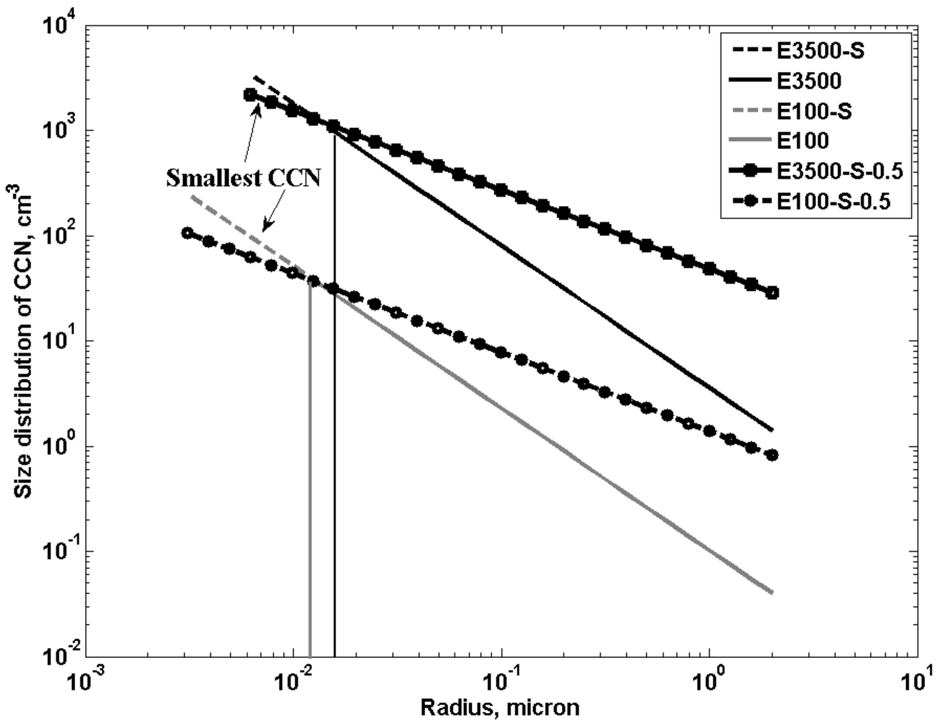

485

486 **Figure 1.** The initial size distributions of aerosols near the surface in different simulations.

487

488

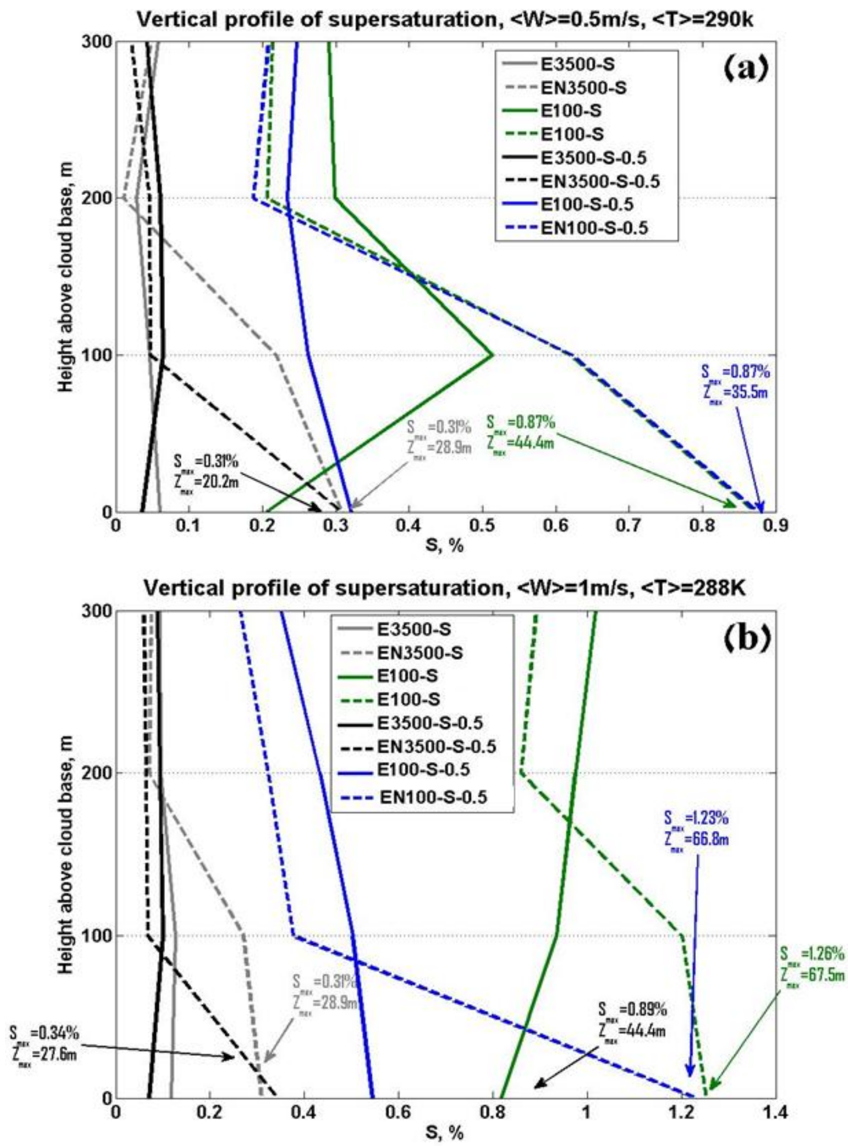

Figure 2. Vertical profiles of the maximum supersaturation above cloud base in several cases. The comparison was conducted under the same average thermodynamic <T> and dynamic <W> conditions. The values of S_{max} and of Z_{max} (the height above cloud base) were calculated according to *Pinsky et al.* [2013].

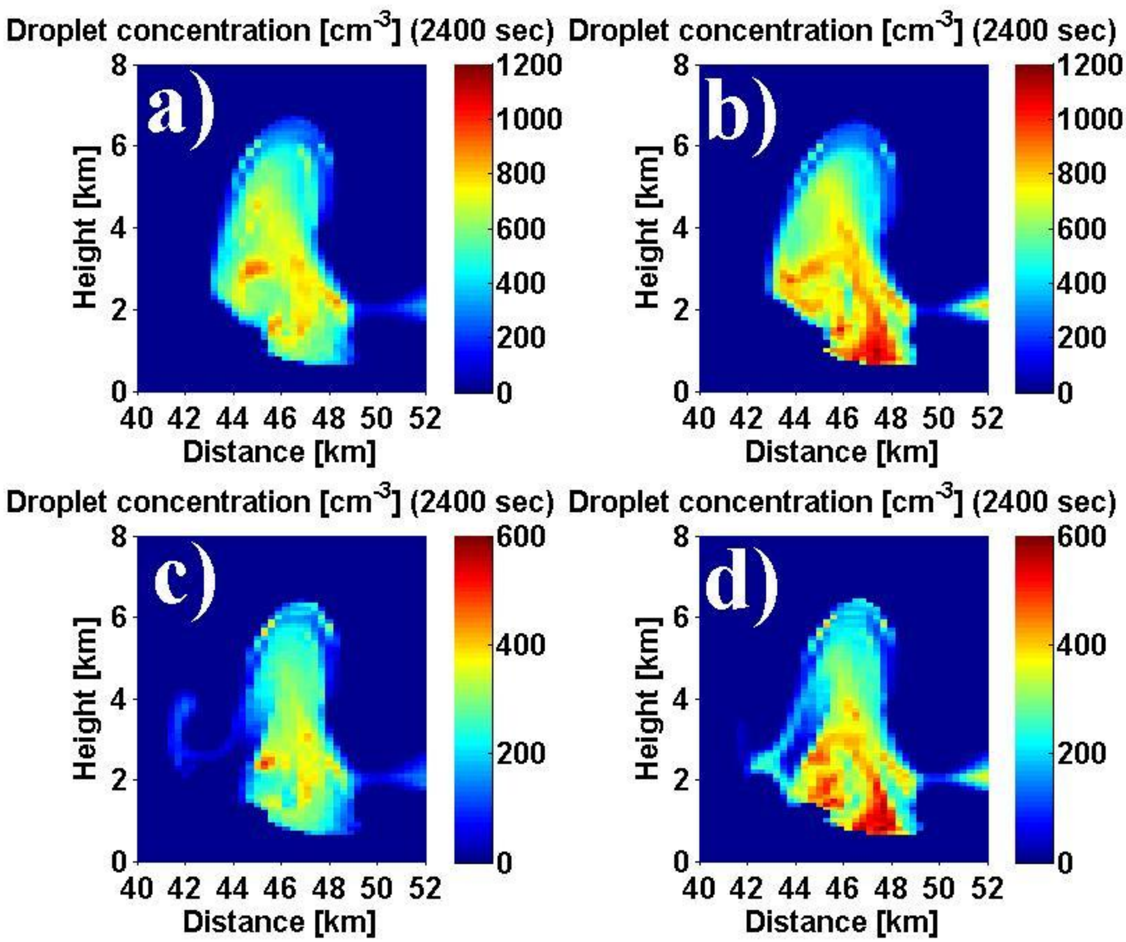

Figure 3. Field of droplet concentration at t=2400s in (a) E3500-S-0.5, (b) EN3500-S-0.5, (c) E3500-S and (d) EN3500-S.

Atmos. Chem. Phys. Discuss., doi:10.5194/acp-2016-499, 2016
Manuscript under review for journal Atmos. Chem. Phys.
Published: 8 July 2016

Atmospheric Chemistry and Physics
Discussions
Open Access

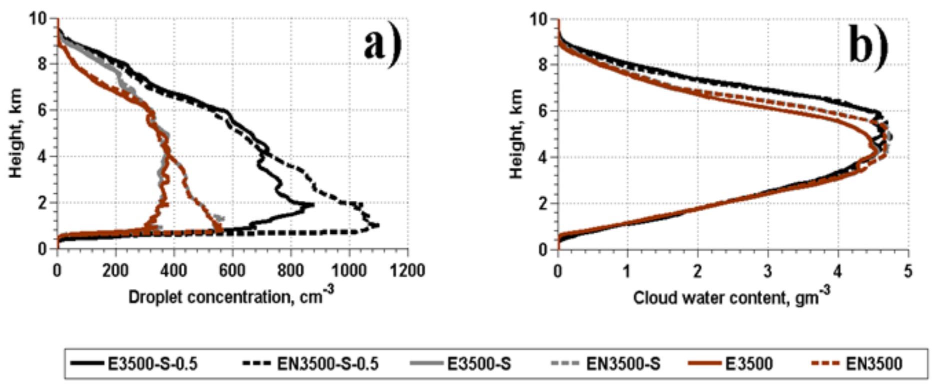

Figure 4. Vertical profiles of the maximum values of (a) droplet concentration and (b) CWC in simulations with high CCN concentration ($N_0 = 3500\ cm^{-3}$). The profiles are obtained by averaging over the time period of 2400-3000s.

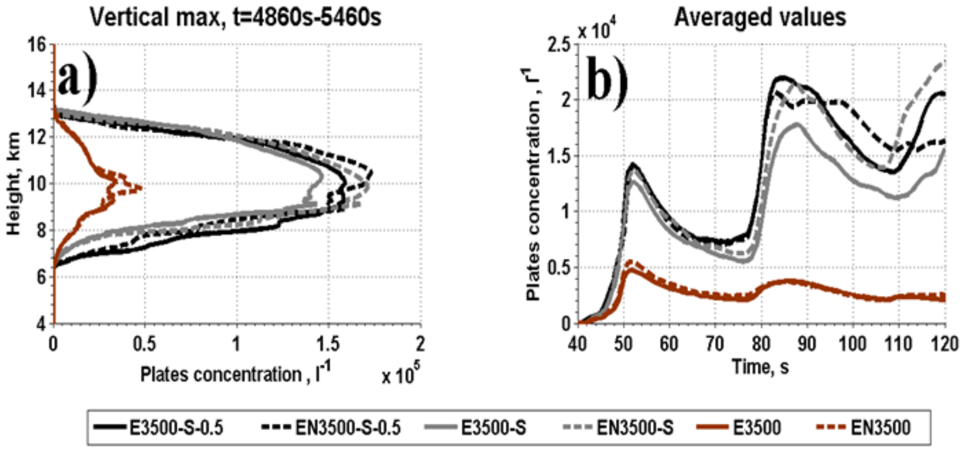

Figure 5. Vertical profiles of (a) maximum values of plates concentration and (b) time dependencies of averaged plate concentration. The profiles are obtained by averaging over the time period of 4860-5460s.

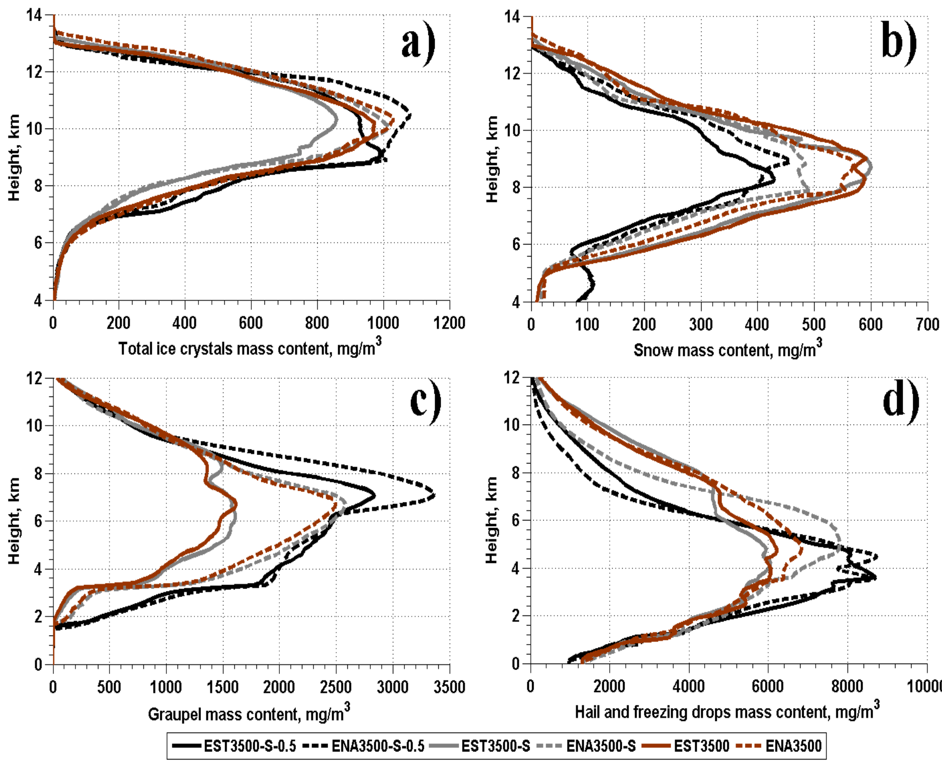

Figure 6. Vertical profiles of the maximum values of mass content: (a) total ice crystals, (b) snow, (c) graupel and (d) total hail and freezing drops in simulations with high CCN concentration ($N_0 = 3500\ cm^{-3}$). The profiles are obtained by averaging over the time period of 4860-5460s.

Atmos. Chem. Phys. Discuss., doi:10.5194/acp-2016-499, 2016
Manuscript under review for journal Atmos. Chem. Phys.
Published: 8 July 2016

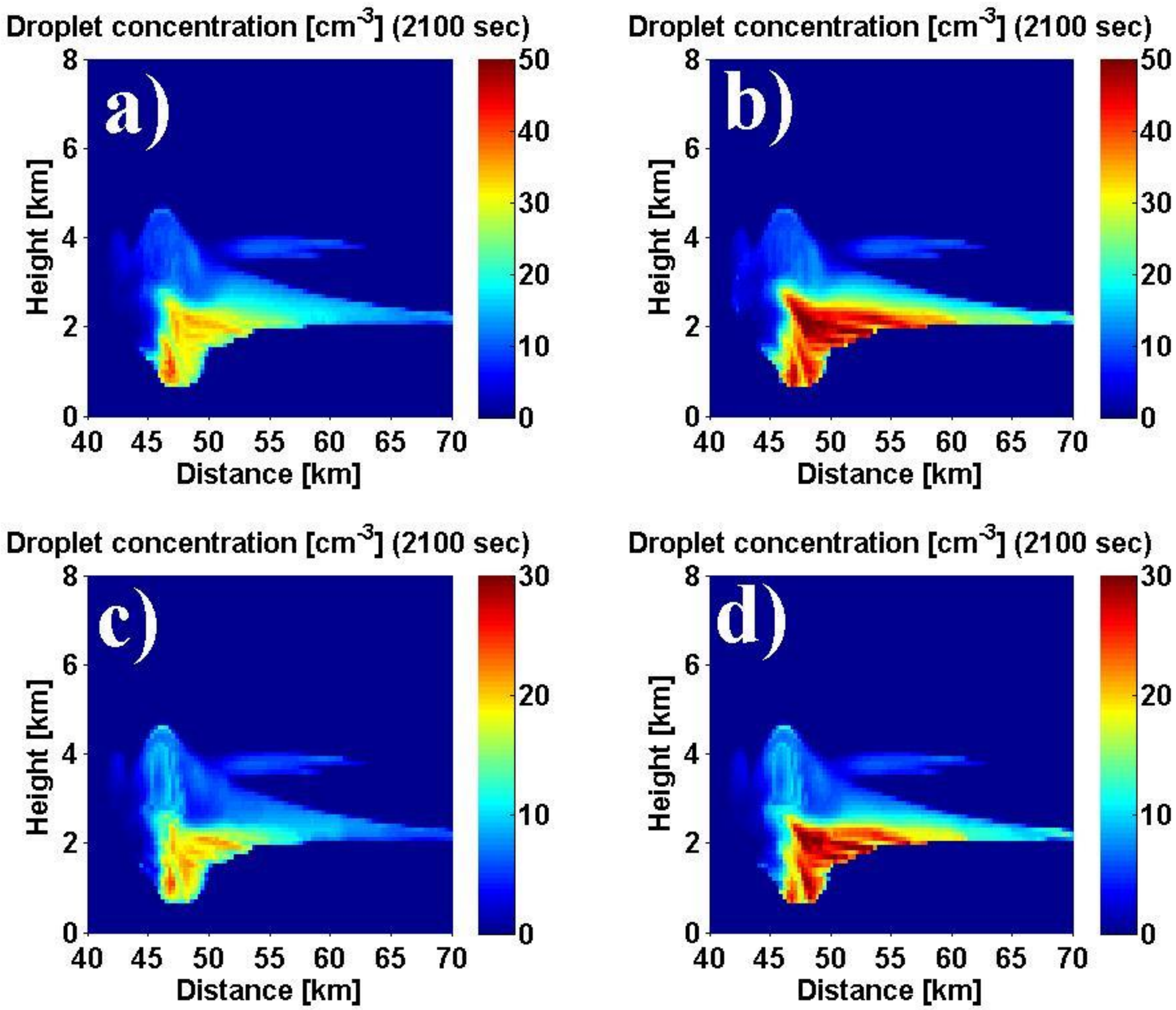

Figure 7. Field of droplet concentration at t=2100s in (a) E100-S-0.5, (b) EN100-S-0.5, (c) E100-S and (d) EN100-S simulations.

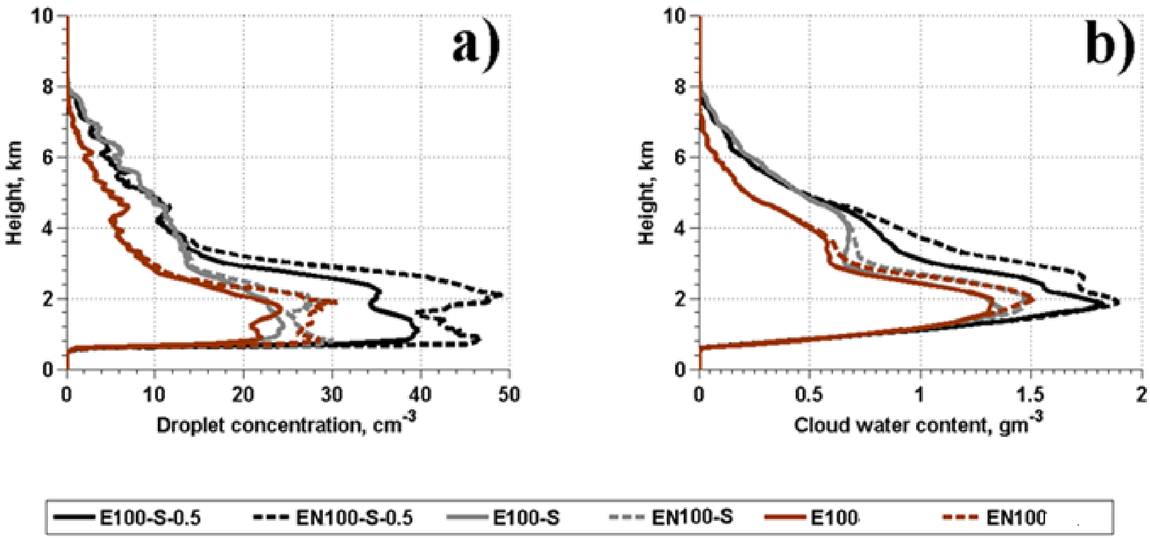

Figure 8. Vertical profiles of the maximum values of droplet concentration (a) and CWC (b) in simulations with low CCN concentration ($N_0 = 100\ cm^{-3}$). The profiles are obtained by averaging over the time period of 2100-2700s.

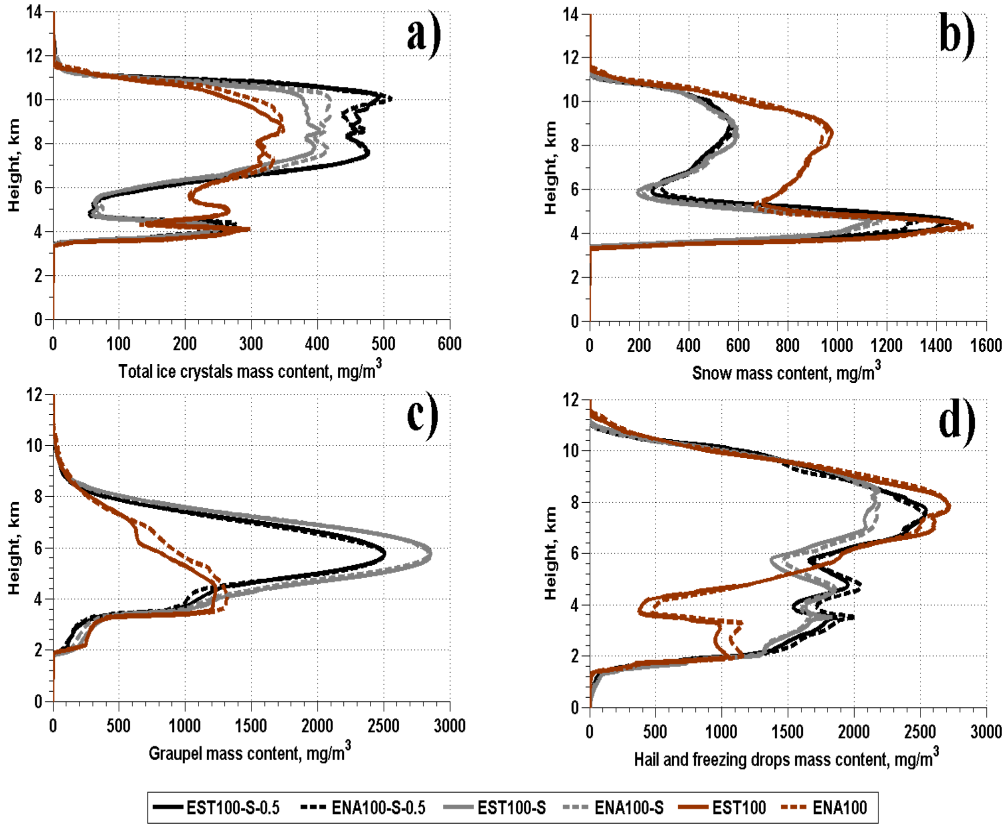

Figure 9. Vertical profiles of the maximum values of mass content: (a) total ice crystals, (b) snow, (c) graupel and (d) total hail and freezing drops in the simulations with high CCN concentration ($N_0 = 100\ cm^{-3}$). The profiles are obtained by averaging over the time period of 3420-4020s.

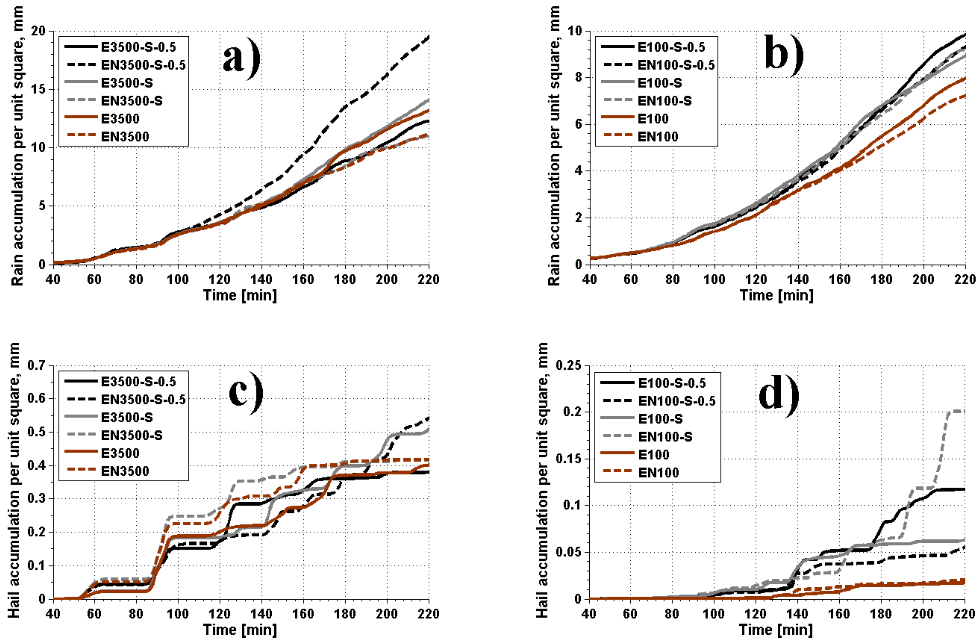

Figure 10. Time dependencies of (a) accumulated rain at surface for polluted and (b) for clean. Accumulated hail at the surface for polluted (c) and for clean (d) in different simulations in polluted cases.